ISSN 2176-5480

22nd International Congress of Mechanical Engineering (COBEM 2013)
November 3-7, 2013, RibeirãoPreto, SP, Brazil

THE EFFECT OF FOOTPRINT ORIENTATION ON THE PERFORMANCE OF A HEAT SPREADER BASED ON FLOW BOILING INSIDE MICRO-SCALE CHANNELS

Hugo L. S. L. Leão
Cristian A. Chávez
Gherhardt Ribatski
Department of Mechanical Engineering, Escola de Engenharia de São Carlos (EESC), University of São Paulo, São Carlos, Brazil
ribatski@sc.usp.br; hugoleao@sc.usp.br; crchavez@usp.br

Abstract. *This paper describes an experimental study about the effect of the footprint orientation on the performance of a microchannels heat sink during flow boiling. The heat sink posses a footprint area of 15x15 mm^2 and contains fifty parallel microchannels with cross-sectional dimensions of 100x500 μm, and total length of 15 mm. The fins between consecutive channels are 200 μm. Experiments were performed for R245fa, mass velocities from 400 to 1000 kg/m^{2}s, heat fluxes up to 320 kW/m^2, liquid subcooling at the heat sink inlet plenum of 5 and 10 °C, saturation pressure of 180kPa. The heat sink performance was evaluated with its footprint area positioned (i) horizontally and (ii) vertically with the microchannels aligned horizontally. A large bubble concentration in the lower part of the heat sink was observed for the configuration (ii). The excess of superheating for onset of nucleated boiling was found independent of the experimental condition. The average heat transfer coefficient was lower for the footprint area positioned vertically. Heat transfer coefficients up to 32 kW/m^{2}K were obtained. The degree of diminishment of the heat transfer coefficient due to the heat sink orientation increases with increasing mass velocity and liquid subcooling. The pressure drop was higher for the heat sink positioned vertically. Therefore, the horizontal orientation of the heat sink footprint provided the best performance in terms of maximizing heat transfer coefficient and minimizing pressure drop.*

Keywords: *Heat Transfer, Flow Boiling, Orientation, Microchannels, Heat Sink*

1. INTRODUCTION

Heat spreaders based on flow boiling mechanism inside micro-scale channels has been a great alternative to dissipate high heat amount in electronic devices because of their compactness and excellent heat transfer performance. According to Ribatski et al. (2007) and Qu and Mudawar (2003), one of the advantages of heat sinks based on flow boiling in microchannels compared to the competing cooling technologies is the combination of high surface area in direct contact with the refrigerant, and high heat transfer coefficients due the flow boiling mechanism. Moreover, evaporation in microchannels minimizes temperature gradient along the heat sink length when compared against single-phase cooling. These characteristics permit minimizing the heat exchanger size and its amount of material. Additionally, the refrigerant inventory is also reduced. Nonetheless, despite of the broad number of studies concerning heat sinks based on flow boiling in microchannels, the knowledge of the boiling heat transfer mechanisms is still limited according to Agostini and Thome (2005), Zhang et al. (2005a), Zhang (2005b) and Harirchian and Garimella(2009).

Tibiriçá and Ribatski (2013) have identified distinct behaviors of pressure drop and heat transfer during flow boiling in micro-scale channels when studies from different laboratories are compared. Additionally, the main heat transfer mechanisms prevailing during flow boiling inside micro-scale channels are still unknown. Ribatski (2012) has also pointed out that flow pattern dynamics in multi-channels are quite different than in single channels. In multichannel configurations, backflows are usually present. The backflows are caused by the fact that bubbles are growing under confined conditions and by the interactions among neighbor channels in the plenum regions. Therefore, the inlet plenum configuration may affect the flow boiling topology and its dynamics.

By decreasing the channel dimensions, the ratio between the surface area in contact with the fluid and the heat sink volume comprising the channels increases, then, the surface tension forces becomes prominent as pointed out by Kandlikar (2004). Therefore, it is expected that the effect of gravitational force on two-phase flow distribution becomes negligible for small diameter tubes. As consequence, only few authors have investigated the effect of flow orientation on the thermal-hydraulic performance of heat sinks based on flow boiling in microchannel.

Kandlikar and Balasubramanian (2005) have investigated the effect of gravity during flow boiling in a heat sink composed by six parallel and rectangular microchannels. They evaluated the heat sink performance for horizontal flow, vertical downflow and vertical upflow. They observed similar flow patterns independent of the flow orientation. The presence of reversal flow was observed for the three configurations, however its intensity was most pronounced for vertical downward flows. Lower pressure drops were observed for vertical upward flows. According to Kandlikar and Balasubramanian (2005), horizontal and vertical upward flows provide higher heat transfer coefficient than vertical

downward flows. Zhang et al. (2005a) and Zhang (2005b) have also investigated the effect of the flow orientation on the performance of heat sinks. They conducted flow boiling experiments for a heat sink containing 21 rectangular parallel microchannels positioned according to the following orientations: vertical upflow, vertical downflow, and horizontal flow with the footprint surface facing horizontally. As observed by Kandlikar and Balasubramanian (2005), vertical upflow configuration has provided the best performance presenting the lowest pressure drop, highest average heat transfer coefficient and minimizing flow instabilities.

More recently, Wang et al. (2012) evaluated the effect of flow orientation on the heat sink performance for footprint orientations from -90° (vertical downward) to 90° (vertical upward). Their experiments were performed for a heat sink containing seven rectangular microchannels with hydraulic diameter of 825 μm. Independent of the inclination of the heat sink, they observed that downward flow always promote the degradation of the heat transfer coefficient compared to horizontal flows. Similar performances were observed for horizontal and vertical upward flows. Although presenting non-uniform flow distribution at low mass velocities, the experiments for 45° upward flow have provided higher heat transfer coefficients. It was found that the orientation effects on heat sink thermal performance decreases with increasing mass velocity. From flow visualizations through high-speed movies, Wang et al. (2012) confirms that elongated bubble velocity is higher for upward flows.

Although some investigations were performed concerning the effects of the heat sink orientation related to the gravitational force, the available results are still non-conclusive. The common belief that the effect of gravitational forces on the heat transfer coefficient is negligible in small size channels seems to be not true in case of multi-channel configurations. Therefore, the present work deals with the experimental investigation for different flow orientations of the two-phase flow characteristics, pressure drop and heat transfer coefficient for flow boiling in heat spreader based on microchannel. The experiments were run for R245fa with the footprint area of the heat sink positioned horizontally and vertically (for downwards flow) with the parallel microchannels horizontally aligned. Experimental results were obtained for heat fluxes up to 320 kW/m^2 (based on the footprint area) and saturation temperatures referred to the pressure at the microchannels inlet of approximately 30°C.

2. EXPERIMENTAL APPARATUS AND PROCEDURE

The experimental setup (shown in Fig. 1) is comprised of refrigerant (or test) and ethylene-glycol/water circuits. The ethylene-glycol/water circuit is responsible for condensing and subcooling the test fluid in the refrigerant circuit. The refrigerant circuit comprises a gear micropump to drive the working fluid through the closed loop, a pre-heater to establish the experimental conditions at the inlet of test section, a test section (containing the heat sink), a plate-type heat exchanger to condense the vapor created in the heated sections, and a refrigerant tank.

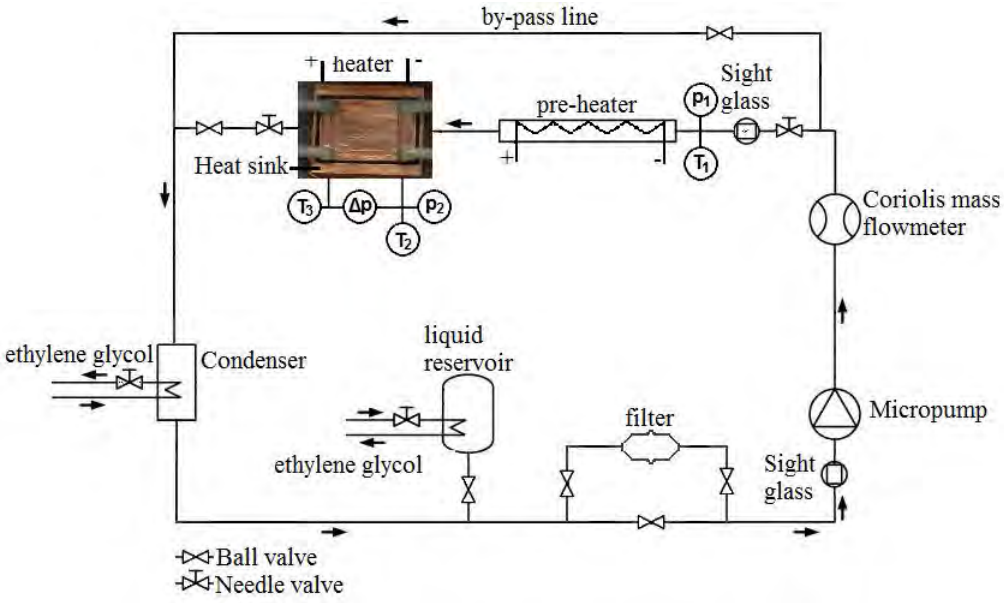

Figure 1. Experimental test loop.

Figure 2 illustrates the test section that consists of a 28x25 mm^2 copper block. The microchannels were made via micro milling process. The heat sink has fifty parallel microchannels with the cross-section dimension of 100μm width, 500μm depth, and total length of 15 mm. The fin present between two consecutive channels has 200μm of width. The heat sink is covered with a Pyrex sheet, allowing high-speed flow visualizations. The inlet and outlet channels were machined in the opposite sides of the Pyrex cover. One additional pair of channels was also machined in the Pyrex sheet in the inlet and outlet plenum regions. Through these channels, the test section is connected to the absolute and

ISSN 2176-5480

differential pressure transducer to measure the pressure at the test section inlet, and the pressure drop along the test section. On the backside of the heat sink, the wall temperature is measured through nine thermocouples embedded within the heat sink wall and distributed according to a 3x3 matrix. The heating effect is obtained through a 0.5 Ω electrical resistance composed by a continuous Kanthal wire bent as a serpentine. The Pyrex sheet, the heat sink, the copper element and the electrical resistance are sandwiched between two pieces of aluminum and sealed with O-rings. The test section is heated by applying a direct DC current to the resistance wire. The test section is thermally isolated from the environment by covering its external surface with elastomeric foam.

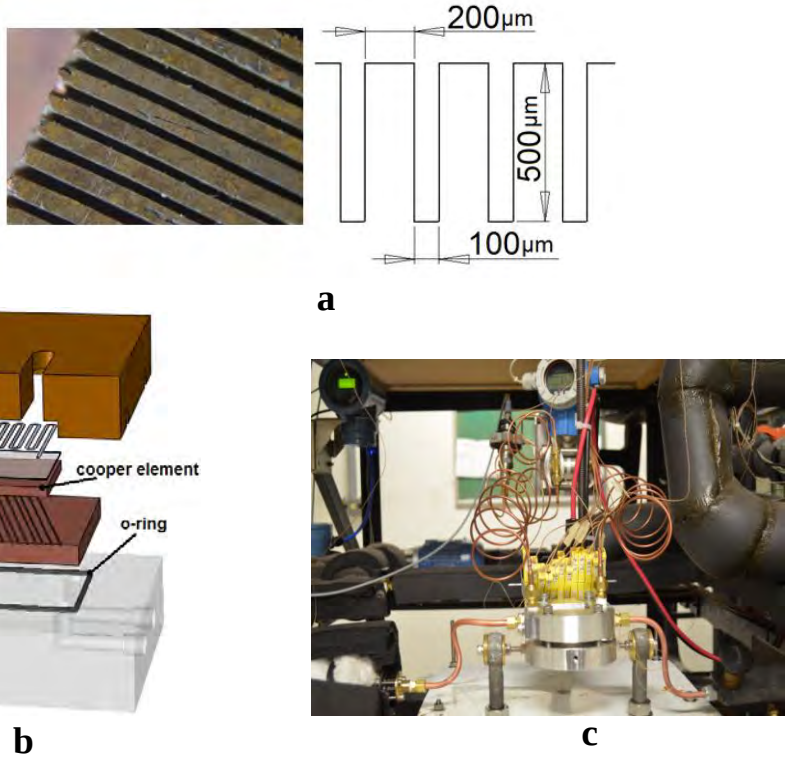

Figure 2. Experimental test section: a) Illustration of the microchannels in the heat spreader; b) Exploded view of the test section (back side view); c) the test section in the experimental apparatus.

Figure 3 shows the orientations according to which the heat sink performances were evaluated. In Fig. 3.a, the heat spreader footprint surface is horizontally positioned (HP) as indicated by the Cartesian coordinate system displaying the y-axis having its direction opposite to the gravitational force, the z-axis having its direction opposite to flow direction and the plane x-z being the footprint surface. Figure 3.b illustrates the heat sink footprint surface vertically positioned (VP) having the parallel microchannels horizontally aligned as indicated by the coordinate system displaying the z-axis having its direction opposite to flow direction, the inlet and outlet plenum region having its direction opposite to the y-axis and the plane y-z being the footprint surface.

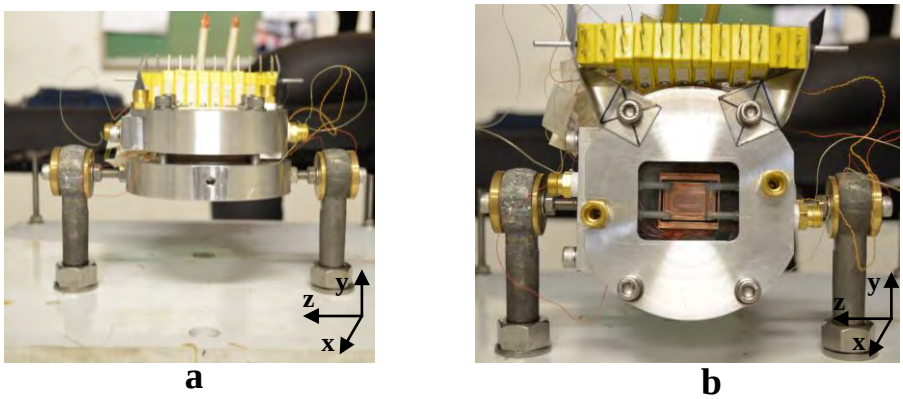

Figure 3. Footprint surface orientation: a) The microchannels heat spreader horizontally positioned (HP); b) The microchannels heat spreader vertically positioned (VP).

The electrical signals measurements were acquired processed and stored by a National Instruments SCXI-1000 chassis with an SCXI 1102 board plate that communicates with the LabVIEW software.

The experiments were conducted first by setting the temperature in the refrigerant tank, which then is kept almost constant by a thermal-controller system. After, the mass velocity is set through a frequency controller acting on the micropump. Then, the temperature at the test section inlet is set by acting on the power supplied to the pre-heater. Tests were conducted by gradually increasing the power supplied to the electrical resistance in the test section, and keeping fixed the remaining experimental parameters. Once the maximum heat flux is attained, the power is gradually decreased.

Experimental results were obtained for the conditions described in Tab. 1.

Table 1. Experimental conditions.

Orientation	Mass Velocity [kg/m^{2}s]	Liquid subcooling [°C]	Heat Flux [kW/m^2]
Horizontal (HP)	400, 600, 800, 1000 and 1200	5 and 10	Up to 320
Vertical (VP)	400, 600, 800 and 1000	5 and 10	Up to 320

3. DATA REDUCTION PROCEDURE

In the present study, the heat flux referred to the footprint area is given as follows:

$$q''_{footprint} = \frac{Q_{real}}{A_{footprint}} \tag{1}$$

where Q_{real} is the electrical power supplied to the Kanthal wire subtracted the heat losses to the environment and the heat transferred to the fluid in the inlet and outlet plenums and $A_{footprint}$ the footprint area (15 x 15 mm^2). The effective heat flux is given by the ratio between Q_{real} and the heated area in contact with the fluid calculated as the product among the heated perimeter, the channels length and the number of channels (50 channels).

Heat losses to the environment were evaluated from single-phase experiments and an average value of 18% was found. The heat transferred in the plenums was estimated based on their superficial area in contact with the fluid, the local temperature of the refrigerant and the heat sink average temperature. For this purpose, the heat transfer correlations of Stephan and Preuber (1979 apud Lee, Garimella and Liu, 2005) and Warrier et al. (2002) were used for single-phase and flow boiling conditions, respectively. In these analyses, it was assumed that heat is transferred only through the copper surfaces. The average wall superheating was calculated as follows:

$$\overline{\Delta T} = \overline{T_{wall}} - \overline{T_{fluid}} \tag{2}$$

where $\overline{T_{wall}}$ is the average temperature of the heat sink based on the measurements of the thermocouples embed within the heat sink wall. The fluid average temperature, $\overline{T_{fluid}}$, is estimated assuming an uniform heat flux along the channels surface and taking into account the subcooled region length, the temperature at the end of the single-phase region and the variation of the saturation temperature with the pressure along the channel length. For single-phase flow experiments along all the channels, the fluid temperature is given as the average temperature between measurements at the inlet and outlet plenums.

The mass velocity is given as the ratio between the mass flow, measured by the Coriolis flow meter, and fifty times the cross sectional area of one single channel (50x100x500 μm^2).

The heat sink averaged heat transfer coefficient is estimated according to the Newton's law of cooling as follows:

$$\bar{h}_{footprint} = \frac{q''_{footprint}}{\overline{\Delta T}} \tag{3}$$

Temperature measurements were calibrated and their uncertainties were evaluated. Accounting for all instrument errors, uncertainties for the calculated parameter were estimated. The experimental uncertainties associated with the sensors and calculated parameters are listed in Table 1.

ISSN 2176-5480

Table 1. Uncertainty of measured and calculated parameters.

Parameters	Uncertainty
H	5 μm
W	5 μm
G	5 μm
T	0.15 K
p	2 kPa
Δp	0.22 kPa
$\overline{T_{wall}}$	0.4 K
$\overline{T_{fluid}}$	0.2 K
q''	0.25 kW/m^2
$\bar{h}$	0.55 kW/m^{2}K

4. RESULTS AND DISCUSSION

The data presented in this paper were obtained by gradually increasing (I) the heat flux until a maximum and then decreasing its value down to zero (D). Figure 4 displays boiling curves for the HP orientation obtained for mass velocities of 600 and 800 kg/m^{2}s, and different degrees of subcooling at the microchannels inlet. Figure 5 presents boiling curves for the VP orientation and a mass velocity of 600 kg/m^{2}s.

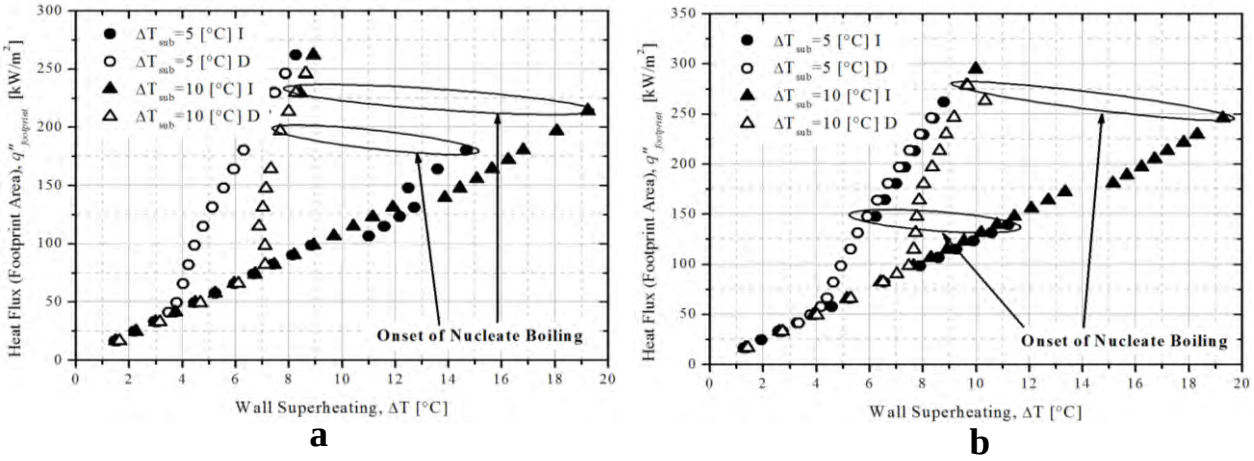

Figure 4. Boiling curves for R245fa with saturation temperature of 30 °C and HP orientation: a) G=600 kg/m^{2}s; b) G=800 kg/m^{2}s, respectively.

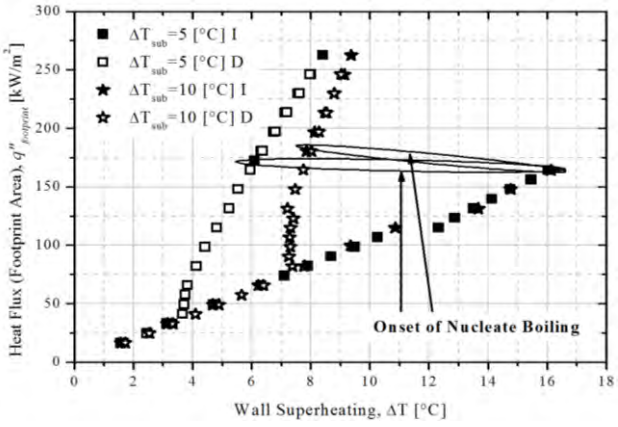

Figure 5. Boiling curves for R245fa with saturation temperature of 30 °C, G=600 kg/m^{2}s and VP orientation.

ISSN 2176-5480

According to the Figs. 4 and 5, the boiling curve moves to the left hand side with decreasing the liquid subcooling. This behavior is related to the fact that the parcel of the heat sink under boiling conditions decreases with increasing the liquid subcooling and the mass velocity. This behavior increases the average wall superheating. Thus, it can be concluded that the decreasing of mass velocity and liquid subcooling causes an augmentation of the dissipated heat flux. It can be also noted that the boiling curves obtained for different degrees of liquid subcooling tend to merge for high wall superheating. Under conditions of gradual heat flux increase (I), a certain superheating excess is necessary to trigger the boiling process (onset of nucleate boiling). This behavior is related to the fact that higher initial superheating is necessary to activate the cavities. For a wall superheating close to 12 ^{o}C and below the ONB, a discontinuity in the boiling curve is occurring. This phenomenon is occurring simultaneously to the occurrence of bubble nucleation in the outlet plenum.

Figures 6 and 7 illustrate comparisons between the boiling curves for VP and HP orientations obtained for mass velocities of 400, 600 and 800 kg/m^{2}s, subcooling degrees of 5 °C and 10 °C. Figures 6 and 7 display only the data obtained under conditions of gradual reduction of heat flux.

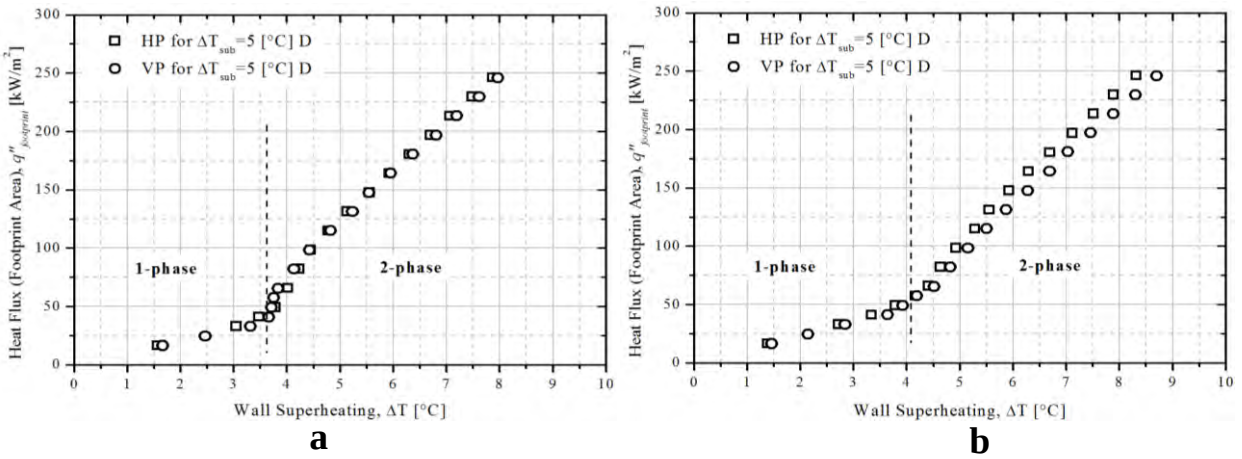

Figure 6. Boiling curves for R245fa with saturation temperature of 30 °C and a liquid subcooling of 5 °C: a) G=600 kg/m^{2}s; b) G=800 kg/m^{2}s.

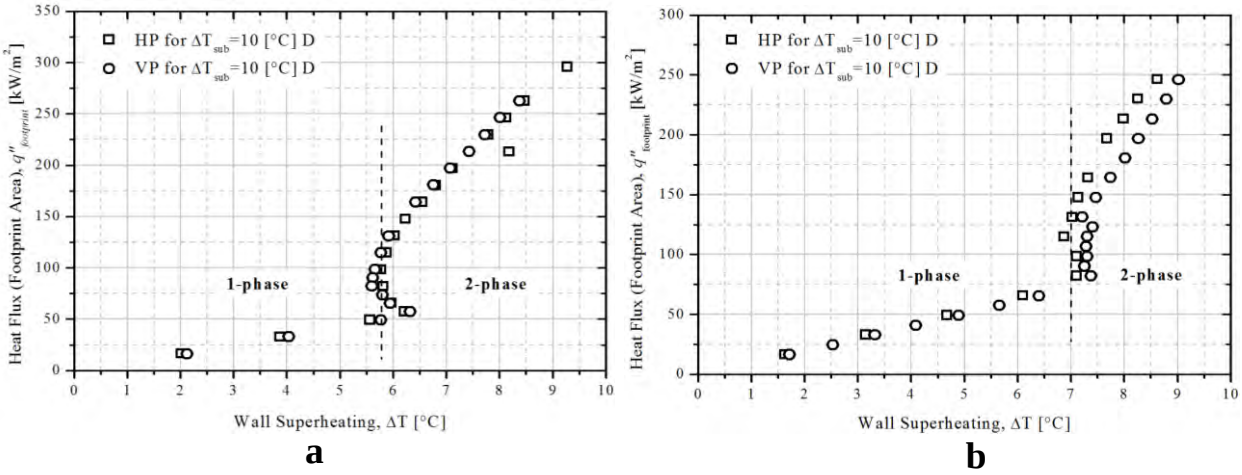

Figure 7. Boiling curves for R245fa with saturation temperature of 30 °C and a liquid subcooling of 10 °C: a) G=400 kg/m^{2}s; b) G=600 kg/m^{2}s.

According to Figs. 6b and 7b, for mass velocities of 800 kg/m^{2}s and 600 kg/m^{2}s, respectively, and under boiling conditions, the HP orientation provides a better performance than the VP orientation. From high-speed movies, it was noted that the degree of non-uniformity of the two-phase flow distribution is higher for the VP orientation and highest mass velocities. In this case, the channels located on the upper part of the heat sink, and closer to the inlet plenum, are mostly filled with liquid while the channels in the lower region of the heat sink present a larger concentration of bubbles. It can be speculated that the higher bubble concentration reduces the mass flow through the lower channels, degrading the heat transfer coefficient. This behavior is enhanced by augmenting the liquid subcooling which causes an increasing of the difference between VP and HP boiling curves. In case of low mass velocities and for the HP configuration, the bubble nucleation becomes uniform among the channels, what promotes a better liquid distribution.

ISSN 2176-5480

Figures 8 and 9 show the same results displayed in Figs. 6 and 7, however in this case according to curves showing h vs. q. For a fixed heat flux and single-phase flow along the channels, the average heat transfer coefficient is not affected by the degree of liquid subcooling and has its value increased with increasing mass velocity. Under the presence of flow boiling along the channels, the heat transfer coefficient increases with decreasing the mass velocity and decreasing the degree of liquid subcooling. According to Figs. 8 and 9, the heat sink vertically positioned with the microchannels horizontally aligned provides a lower average heat transfer coefficient than the heat sink horizontally oriented. The detrimental performance of the VP orientation increases with increasing mass velocity and liquid subcooling.

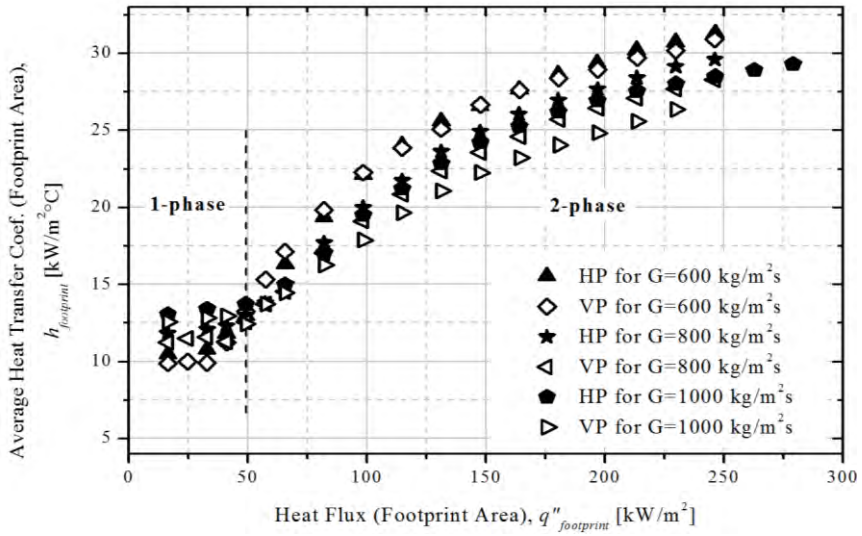

Figure 8. Illustration of the Effects of mass velocity and footprint orientation on heat sink averaged heat transfer coefficient for R245fa with liquid subcooling of 5 °C and saturation temperature of 30 °C.

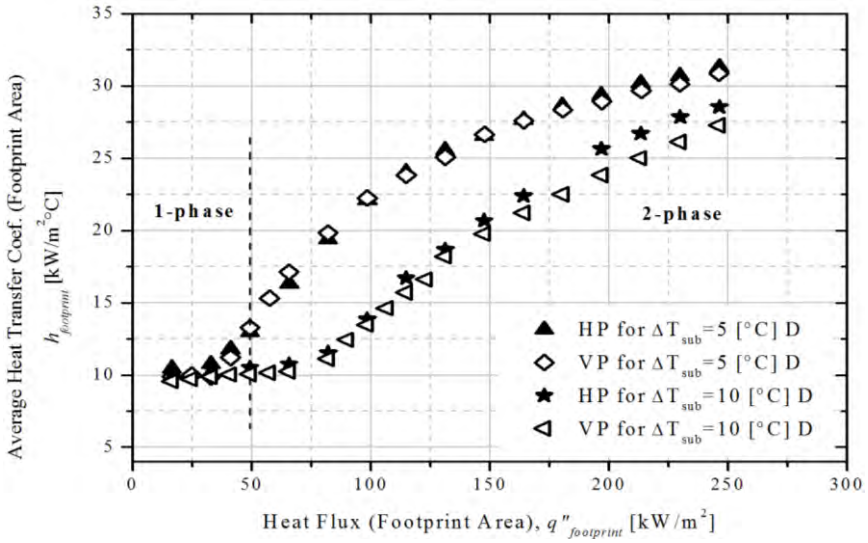

Figure 9. Illustration of the effect of liquid subcooling and footprint orientation on the heat sink averaged heat transfer coefficient for R245fa with saturation temperature of 30 °C and mass velocity of 600 kg/m^{2}s.

Figure 10 illustrates the effects of mass velocity, heat flux, and heat sink orientation on the total pressure drop along the microchannels. Under the presence of flow boiling, it is noted in Fig. 10 that the total pressure drop increases with increasing heat flux and mass velocity. This behavior already expected is mainly due to the increase of the frictional parcel of the pressure drop with increasing the two-phase flow velocity. According to Fig. 10, the VP heat sink orientation provides higher pressure drops than the HP orientation under similar experimental conditions. The total pressure drop difference between VP and HP orientations increases with increasing mass velocity, liquid subcooling and heat flux. Such a behavior is due to the higher degree of non-uniformity of the two-phase flow among the channels

for the VP orientation, which, according to the two-phase flow images, increases with increasing mass velocity, heat flux and liquid subcooling.

Therefore, based on the pressure drop and heat transfer behaviors for both heat sink orientations, it can be concluded that the heat sink horizontally positioned provides a better performance than the vertical position with the microchannels horizontally aligned. Finally, it can be highlighted the importance of the designing of the inlet manifold of the heat sink in order of attaining an uniform two-phase flow distribution among the channels, and, so minimizing pressure drop and maximizing heat transfer.

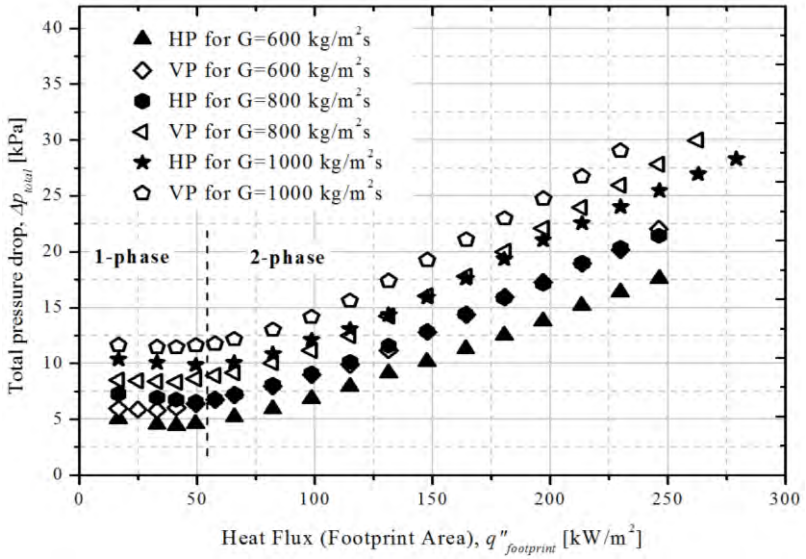

Figure 10. The effect of mass velocity, heat flux and heat sink footprint orientation on the total pressure drop across the microchannels for R245fa with saturation temperature of 30 °C and a liquid subcooling of 5 °C.

5. CONCLUSION

New heat transfer data were obtained for R245fa in a heat sink positioned according to two footprint surface orientations. Flow boiling heat transfer coefficients up to 32 kW/m^2°C were achieved. The experimental data were analyzed and the main heat transfer trends were discussed. From this study, the following main conclusions can be drawn:

- An excess of superheating was necessary to trigger the boiling process (onset of nucleate boiling) along the microchannels. Under boiling conditions along the microchannels and for the same wall superheating, decreasing the mass velocity and liquid subcooling promotes the augmentation of the amount of heat dissipated;
- In general, the heat sink operating according to the HP orientation provides a better heat transfer behavior due to the presence of a better two-phase flow distribution;
- Under flow boiling conditions along the microchannels, the heat transfer coefficient increases with decreasing mass velocity and the liquid subcooling;
- The VP heat sink orientation provides higher pressure drops than the HP orientation under similar experimental conditions;
- The heat sink horizontally positioned provides a better overall performance than the vertical position with the microchannels horizontally aligned.

6. ACKNOWLEDGEMENTS

The authors gratefully acknowledge the financial supports under Contracts numbers 576982/2008-3 given by CNPq, (The National Council for Scientific and Technological Development, Brazil) 2011/50176-2 given by FAPESP (São Paulo Research Foundation) and the research grant given by CAPES (Coordination for the Improvement of Higher Level Personnel). The technical support given by Mr. José Roberto Bogni is also appreciated and recognized.

7. REFERENCES

Agostini, B. and Thome, J.R., 2005. "Comparison of an extended database of flow boiling heat transfer coefficient in multi-microchannel elements with the three-zone model". in: *Proc. ECI International Conference on Heat Transfer and Fluid Flow in Microscale,* CastelvecchioPascoli, Italy.

Do Nascimento, F.J., Leão, H.L.S.L. and Ribatski, G., 2013. "An experimental study on flow boiling heat transfer of R134a in a microchannel-based heat sink". *Experimental Thermal and Fluid Science*, Vol. 45, pp. 117-127.

Harirchian, T. and Garimella, S.V., 2009. "Effects of channel dimension, heat flux, and mass flux on flow boiling regimes in microchannels". *International Journal of Multiphase Flow*, Vol. 35, pp. 349-362.

Intel, C., 2012. "Products datasheet". accessed 16 feb. 2012, <http://www.intel.com>.

Kandlikar, S.G. and Balasubramanian, P., 2005. "An experimental study on the effect of gravitational orientation on flow boiling of water in 1054 x 197μm parallel minichannels". *Journal of Heat Transactions – T ASME*, Vol. 127, pp. 820-829.

Qu, W. and Mudawar, I., 2003. "Flow boiling heat transfer in two-phase micro-channel heat sinks–I. Experimental investigation and assessment of correlation methods". *International Journal of Heat and Mass Transfer*, Vol. 46, pp. 2755-2771.

Ribatski, G., 2012. "A Critical overview on the recent literature concerning flow boiling and two-phase flows inside microscale channels", in: *International Conference on Boiling and Condensation Heat Transfer*, Lausanne, Switzerland.

Ribatski, G., Navarro, H.A., Cabezas-Gómez, L. and Saíz-Jabardo, J.M., 2007. "The advantages of evaporation in micro-scale channels to cool microelectronic devices". *Thermal Engineering*, Vol. 6, pp. 34-39.

Lee, P.-S., Garimella, S. V. and Liu, D., 2005. "Investigation of heat transfer in rectangular microchannels". *International Journal of Heat and Mass Transfer*, Vol. 48, pp. 1688-1704.

Tibiriçá, C.B. and Ribatski, G., 2013. "Flow boiling in micro-scale channels–Synthesized literature review". *International Journal of Refrigeration*, vol. 36, pp. 301-324, 2013.

Wang, C.H., Chang, W.J., Dai, C.H., Lin, Y.T. and Yang, K.S., 2012. "Effect of inclination on the convective boiling performance of a microchannel heat sink using HFE-7100". *Experimental Thermal and Fluid Science*, Vol. 36, pp. 143-148.

Warrier, G. R., Dhir, V. K. and Momoda, L. A., 2002. "Heat transfer and pressure drop in narrow rectangular channels". *Experimental Thermal and Fluid Science*, Vol. 26, pp. 53-64.

Zhang, H.Y., 2005b. "Flow boiling heat transfer in microchannel heat sinks of different flow orientations", in: *Proceedings of the ASME Summer Heat Transfer Conference*, Singapore, pp. 859–866.

Zhang, H.Y., Pinjala, D. and Wong, T.N., 2005a. "Experimental characterization of flow boiling heat transfer in microchannel heat sinks with different flow orientations". in: *IEEE – Electronics Packaging Technology Conference*, pp. 670–676.

8. RESPONSIBILITY NOTICE

The author(s) is (are) the only responsible for the printed material included in this paper.